IECC 2018

sciforum

Conference Proceedings Paper

Intermolecular Interactions Required for the Formation of Liquid Microcrystals Produced by the Precursors Self-Organized from Protonated TPP Dimers

Alexander Udal'tsov

Faculty of Biology, Lomonosov Moscow State University, Vorobjovy Gory 12, 119234 Moscow, Russia; avu151@yandex.ru; Tel.: +7-926-542-1322

Abstract: Features of solute-solvent intermolecular interaction establishing hydrogen bonds were studied in view of proton sharing in the O---H^+–O moiety is the prerequisite for proton moving through water. Liquid microcrystals are expected to be formed due to the protons moving through water confined in their precursors. Among the different oxygen-containing organic solvents well-dissolved in water, tetrahydrofuran (THF) has been found the most suitable since it forms a molecular complex with carbon dioxide dissolved in water producing the ions H^+ and $(HCO_3)^-$. This three-component complex exhibits in infrared spectra vibrational bands characterizing the complex and the proton sharing in the O---H^+–O moiety. Assemblies consisting of water with 0.86 mol·L^{-1} THF and mono-protonated *meso*-tetraphenylporphine (TPP) dimers self-organized into submicroscopic particles in solution have been investigated by infrared spectroscopy, SEM, and AFM in thin layers. Earlier found tight water covering the submicroscopic particles is proved to exhibit an ordered and non-ordered local areas on the surface. Molecular characteristics estimated for the three-component complex involving THF suggest that the complex partakes in the crystallization process providing protons moving through water together with the TPP dimers.

Keywords: liquid microcrystals; solute-solvent interactions; hydrogen bonding; proton sharing; THF·$(HCO_3)^-$·H_3O^+ complex

1. Introduction

Liquid crystals have a wide application in photonics, sensors, telecommunication, liquid crystal displays, mobile phones, digital cameras, in development of tunable photonic devices, and so on, so many books and publications are devoted to liquid crystals [1–5]. Physical nature of the formation of liquid crystals is usually connected with rod-like organic molecules, which on cooling can change their orientation with the transition from isotropic to anisotropic liquid, wherein hydrogen bonds are often formed between the molecules [5]. Liquid microcrystals can be also formed on the base of self-organized molecular systems consisting of water and a porphyrin dimers, namely *meso*-tetraphenylporphine (TPP) whose molecules are connected to each other in the dimer via hydrogen bonds of small-size protonated water cluster [6]. The latter mode seems to be very perspective because the engineering of liquid nanocrystals is possible too that may be depending on the physical nature of liquid crystal formation. Such nanocrystals are very likely found in thin layer earlier [7]. In this connection, the physical nature of the formation of liquid crystals, micro- and nano-crystals acquires important significance for future development of the research field. New developments based on liquid crystals considerably extend the application area [8], but the physical nature of the liquid crystal phenomenon is remained unclear. The understanding of this phenomenon on

molecular level is extremely desirable to outline all applications of the liquid crystals of a wide range of their size. The findings of key role of water in the crystalliazation of the self-organized assemblies of protonated TPP dimers and Zundel cation (H_2O---H^+–OH_2) operation [6,9] imply the formation of liquid crystal state due to proton moving through water confined in the assemblies. However, role of water-soluble organic solvent was remained unclear because the organic solvent was expected to be evaporated together with the excess of hydrochloric acid and water. Thus, the work was aimed on elucidation of the role of water-soluble organic solvent in the processes of liquid crystals formation including the study of the solute-solvent interactions separately using infrared spectroscopy.

2. Results

Thin layers of different solvents well-dissolved in water were tested by IR spectroscopy to elucidate features of the solute-solvent molecular interactions, since the organic solvent influences on the morphology of the self-assembled domains [10].

2.1. Infrared Spectroscopy of Solvents and Submicroscopic Particles Consisting of TPP Dimers and Water

Among the organic solvents such as dioxane, dimethylformamide, tetrahydrofuran (THF), and acetic acid, the IR spectra of THF containing water were found the most interesting, thin layers of which exhibit three-peaked bands around 2344, 2680, and 3508 cm^{-1} shown in Figure 1. Obviously the band at 2344 cm^{-1} testifies the presence of atmospheric CO_2 dissolved in water, the other at 3508 cm^{-1} characterize O–H stretching vibrations, and the band at 2680 cm^{-1} is the evidence of proton sharing in the O---H^+–O moiety [7]. As known, CO_2 dissolved in water can produce H^+ and $(HCO_3)^-$. The band of H–O–H bending vibration around 1634 cm^{-1} is red shifted by 8–10 cm^{-1} in Figure 1 relatively that at 1640 cm^{-1} indicating a stronger hydrogen bonding in THF/water solution than in pure water.

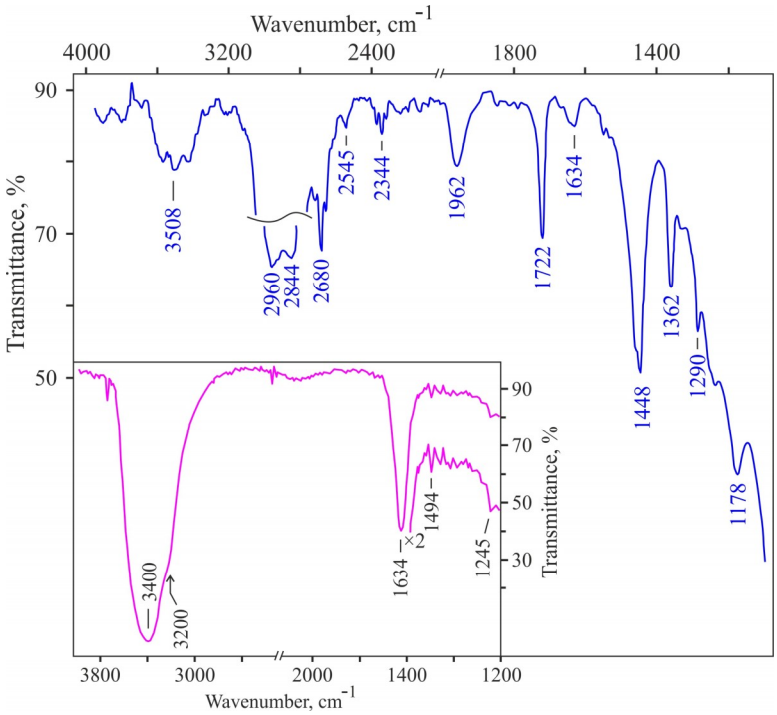

Figure 1. Infrared spectrum of THF containing water, a drop crashed between CaF_2 plates (left-upper scale); the 1722 cm^{-1} band attests the presence of $H^+(HCO_3)^-$ in the solution. Inset shows IR spectrum obtained after full evaporation of 3.6 mol L^{-1} aqueous THF in the presence of 0.4 N HCl in the solution producing the lustreless spot, which during 5-10 sec absorbs water vapor from air forming the aqueous surface on CaF_2 plate (right-lower scale).

Such solvents as THF and aqueous hydrochloric acid are known as well-evaporating liquids. Their solution gives a lustreless spot after the complete evaporation, however the spot was almost instantaneously transformed into liquid, IR spectrum of which is shown in Figure 1, inset. The main bands of the letter are O–H stretch at 3400 cm^{-1} of water with a shoulder around 3200 cm^{-1} and H–O–H bend at 1634 cm^{-1}. The small bands attest the features of local interactions between the molecules. The shoulder around 3200 cm^{-1} matches the small three-peaked band at 3207 cm^{-1} observed in the spectrum in Figure 2 of THF containing water. Thus, a complex formed by THF and CO_2 dissolved in water, structure of which is depicted in Figure 2, inset according to characteristic bands around 2344, 2680, and 3508 cm^{-1}, is present in THF containing water.

The oxygen-oxygen distance ($R_{O–O}$) in the O---H^+–O moiety of the complex can be evaluated with a correlation obtained for small-size water clusters, where ω is the observed wavenumber [11].

$$\omega = 6205 \times R_{O–O} - 13107 \quad (1)$$

With ω = 2680 cm^{-1} of the three-peaked band characterizing proton sharing displayed in Figure 2, inset (below) the calculated $R_{O–O}$ = 2.54 Å that is close to 2.56 Å found earlier for the N–O distance in the N–H---O moiety of the protonated water cluster embedded between TPP units in the dimer [7].

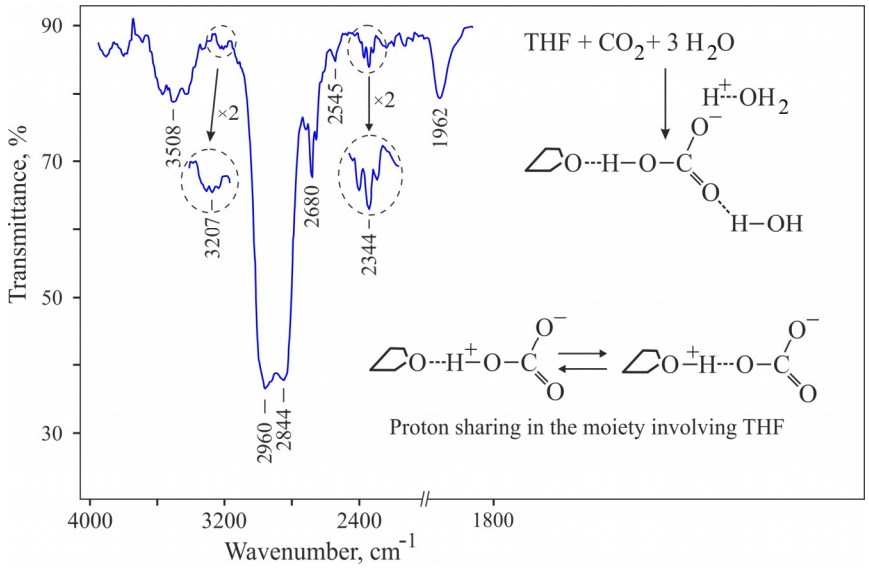

Figure 2. Infrared spectrum of THF containing water with enlargements of local regions, a drop crashed between CaF_2 plates. Insets show formation of the complex with carbon dioxide dissolved in water (upper); and proton sharing in the moiety containg THF (below) that provides proton moving through water.

The three-component complex is also formed in the presence of hydrochloric acid, the lustreless spot of which is proved very hygroscopic. However, in the presence of HCl the complex contains non-dissociated carbonic acid instead of bicarbonate ion. The Cl^- ion is most likey does not involved in the structure of the complex as depicted in Figure 2, inset.

A doublet nearby 1000 cm^{-1} observed in IR and resonance Raman spectra of self-assembled mono-protonated TPP dimers has been identified with proton sharing in the N–H_3O^+---O moiety [9]. The resonance structures corresponding to the components of the resonance Raman spectrum displayed in Figure 3 illustrate the change of the hydrogen bond location in N–H_3O^+---OH_2 under the proton moving. As we can see, the peaks at 1000 and 1025 cm^{-1} differ from each other that implies somewhat different localized states, whose characteristics can be evaluated (see below).

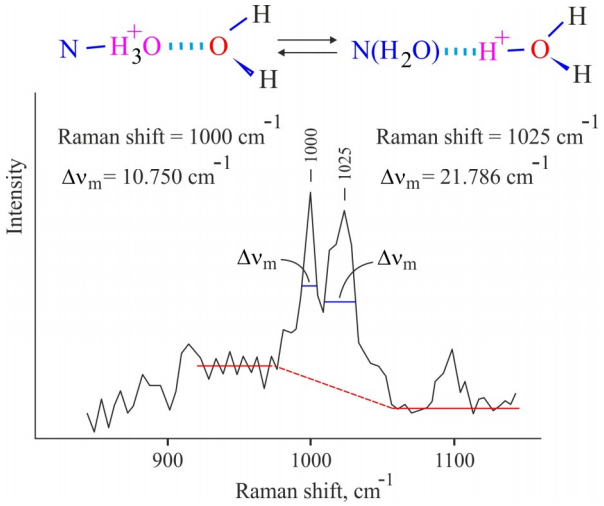

Figure 3. Resonance Raman spectrum of *meso*-tetraphenylporphine dimers, $(TPPH)_2^{2+}$ that exhibits λ_{max} = 437 nm in 50% aqueous acetone (v/v) (λ_{ex} = 441.6 nm, a spectral slit width for the registration was 4 cm^{-1}, He-Cd laser [12]). Inset shows the illustration of proton motions in the $N–H_3O^+$---O moiety of the protonated water cluster embedded between TPP units in the dimer [7].

The effect of the support of the self-assembled mono-protonated TPP dimers found earlier in IR spectra [12] is shown in Figure 4. On the solid CaF_2 plate, the bands of water confined in the assemblies of the TPP dimers are strongly narrowed in comparison with those on liquid support of oil. This effect has been discussed earlier [12] and it should be noted that the amplitude of the vibrations in the quasi-crystal structure are strongly restricted, while proton moving through the confined water can take place most likely in both cases because the structure self-organization occurs on the solid support too [6,7].

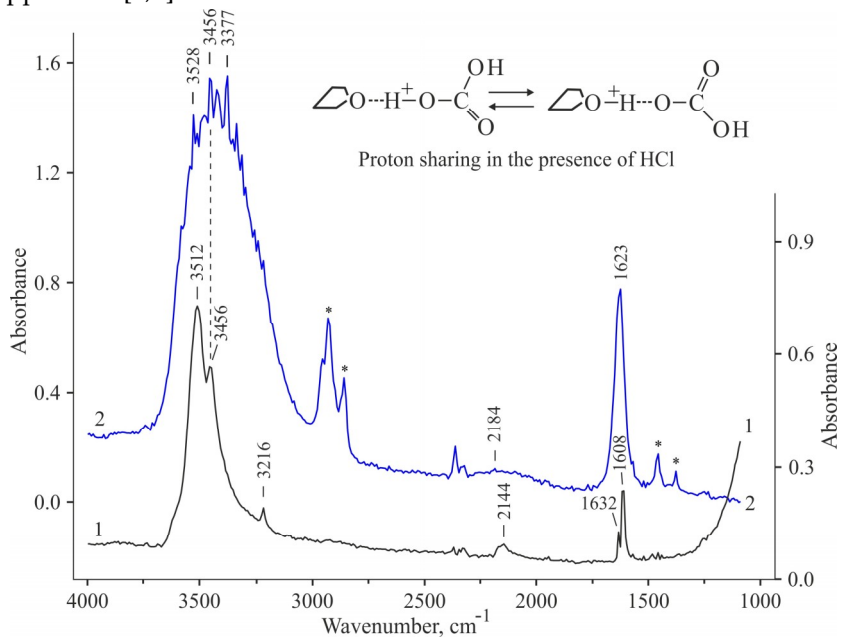

Figure 4. Infrared spectra of mono-protonated TPP dimers self-assembled into submicroscopic particles in 0.86 mol·L^{-1} aqueous THF in the presence of 0.4 N HCl recorded after the solvent evaporation: (1) thin layer on CaF_2 plate (right scale); and (2) the same sample collected from the plate in Vaseline oil (left scale); an asterisk marks the oil bands. The TPP/H_2O molar ratio is approximately 1/600÷1/630 [13].

Thus, the proton sharing that takes place in the complex involving THF and CO_2 dissolved in water provides the intermolecular interactions required for the formation of liquid microcrystals. Note that proton sharing is the prerequisite for proton moving through water confined in the submicroscopic particles or aggregates [9]. This molecular complex and the protonated TPP dimers provide proton moving through water as during the structure self-organization in solution and most likely in the course of the crystallization in thin layer. The other solutions of water with dioxane, dimethylformamide, and acetic acid did not show up similar vibrational characteristics.

2.2. AFM-SNOM of Submicroscopic Particles in Thin Layer Covered by Tight Water

The submicroscopic particles or the particles of microscopic proportions are usually covered by a layer of tight water because a sample tested by non-contact and contact AFM showed up the different images [14]. Non-contact AFM exhibits the particles of microscopic proportions as displayed in Figure 5, while contact AFM of the same sample previously revealed nanoparticles of 200–400 nm size [14]. The simultaneous SNOM image shown in Figure 5 outlines the shape of the particles seen by AFM, but all the particles are completely transparent for the light that is in fair agreement with the TPP/H_2O = 1/600 molar ratio.

The detailed study of the tight water surface as displayed in Figure 6 showed up two different areas, one of them with an ordered structure and the other is non-ordered. The tight water contains a large amount of the salt [14], which is most likely concentrated in the non-ordered areas. Arrows in the AFM image of Figure 6(a) mark the border between these different areas. As found previously, the engineering of microcrystals based on the self-organized protonated TPP dimers requires three acts of the engineering actions for the fabrication of 30–35 μm green crystals [7] and two acts for the microcrystals of ellipsoid shape of ca. 1.7×2.4 μm size measured at a half of the height [6]. One from those actions is the application of gaseous water to initiate the crystallization in order to Zundel cations (H_2O---H^+–OH_2) action in the surface layer could occur [6,7].

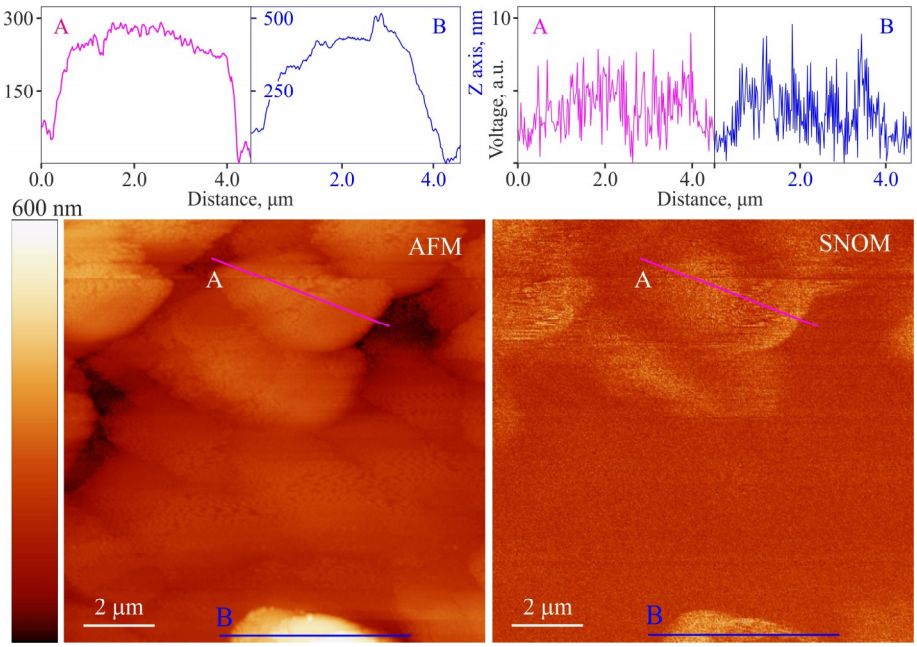

Figure 5. Simultaneous non-contact AFM (10 μm×10 μm), top view, z-scale: 600 nm (to the left) and shear-force SNOM, z-scale: voltage 0.5 V (to the right) scans of a thin layer, which was prepared by solvent evaporation from mainly di-protonated TPP dimers self-assembled in 2 N aqueous HCl with 0.86 mol L^{-1} THF and the cross-sections A and B of different domains of the assemblies.

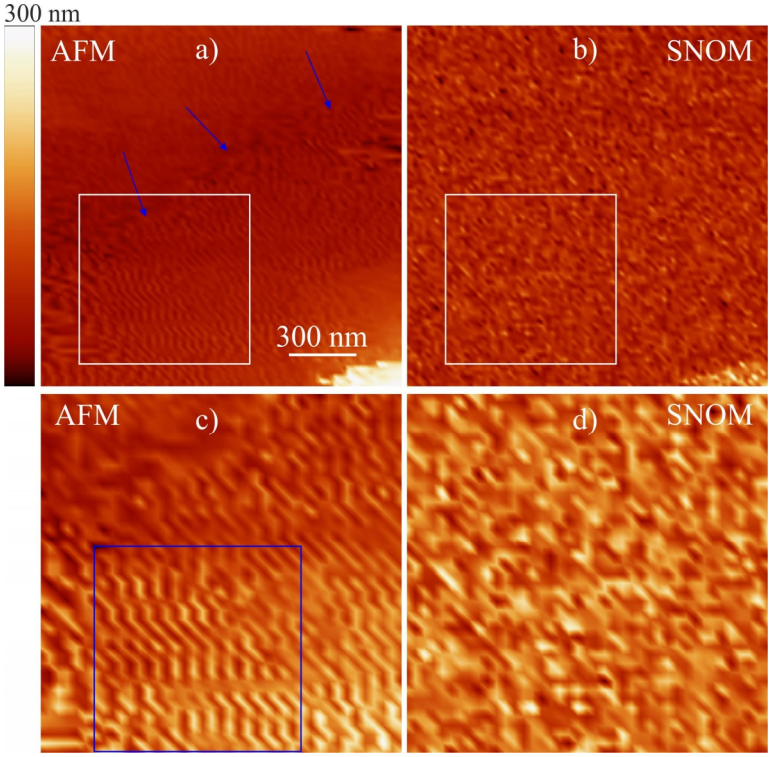

Figure 6. Simultaneous non-contact AFM and shear-force SNOM images (top view) of the thin layer as displayed in Figure 5; AFM: (upper, 1.6 μm×1.6 μm and lower, 0.8 μm×0.8 μm), top view, z-scale: 300 nm (to the left); SNOM: z-scale: voltage 0.2 V (to the right); the SNOM image does not exhibit an ordered area like the AFM image that is why the further study with SNOM did not performed.

The ordered areas apparently contain the salt too but in considerably less amounts because they demonstate crystalline structure as displayed in Figure 7. The cross-section exhibits a regular structure on the surface with the step width of 28.6 nm. It should be noted that the resolution of the measurements was the same as found earlier [15], namely (10.3–10.6)±0.08 nm with the reliability of 99%. The latter admits to consider these ordered areas should not be artifacts, although the finding requires further detail research in the future.

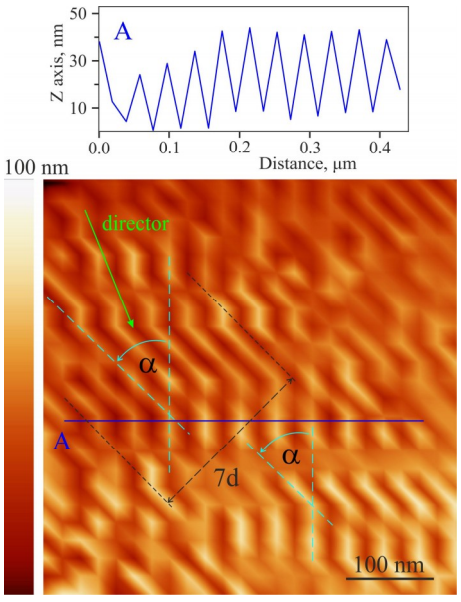

Figure 7. Non-contact AFM image taken from Figure 6c, blue square, 0.5 μm×0.5 μm (top view) with the cross-section; letter marking the cross-section line drawn in the top-view shows the origin of the cross-section here and in Figures 5 and 9; a director indicates forward and backward proton moving directions through water; the sharp angle α = 46.2°; the calculated distance 7d =200 nm, d =28.6 nm; see details in the text.

The invariable sharp angle (α = 46.2°) between the strands can be the next evidence of the reliability of the ordered areas on the surface. Although the latter angle is somewhat different from the theoretical α = 52.4° predicted by the model of proton moving through water [9], but similar deviation has been found for self-assembled mono-protonated TPP dimers with the use of distilled water (see below). Besides, the dissolved carbon dioxide involving THF in the complex does not possess similar hydrophobic affinity like TPP, mono-protonated dimers of which are self-organized due to proton moving through water that results in the experimental angle 55°±3° of a slanting cross on the surface with the use of de-ionized water [9,12].

Thus, the three-component complex formed by hydronium ion (H_3O^+), THF, and carbon dioxide dissolved in water, which has been converted into carbonic acid, should provide proton moving through water too. This complex is located in the tight water covering the submicroscopic particles and exhibits proton sharing in the O---H^+–O moiety like the other one formed in the aqueous THF according to the three-component band at 2680 cm^{-1}.

2.3. Crystallization Process of the Submicroscopic Particle Self-Organized into Domain in Thin Layer

According to theoretical model of proton moving through water via intermediate states with proton sharing between the neighboring water molecules, there is a threshold of the O–O distance of 2.45 Å when the possibilities of proton sharing and its moving through water (or delocalization) are equal [9]. In that model there is also a peculiar assuming that the proton bypasses the neighboring hydrogen-bonded water molecule to explain the sharp angle of (55±3)° between the tracks on the surface like those shown in Figure 8. These tracks are originated because of protons moving along the axis of the aggregate length in the forward and backward directions generating the inner structure self-organization in the water-porphyrin matrix [9]. Therefore, the corresponding director shown in Figure 8 indicates the forward and backward proton moving through water confined in the aggregates.

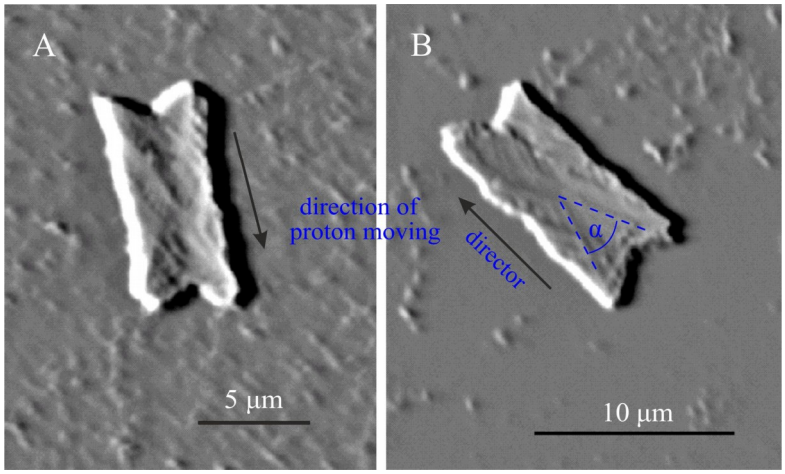

Figure 8. SEM images of the self-organized assemblies containing mainly mono-protonated TPP dimers and water after the removing of weakly bound water by evaporation of 0.86 mol L^{-1} aqueous THF in the presence of 0.4 N HCl: A and B were obtained with somewhat different porphyrin concentrations; the sharp angle α = 43.2°. An arrow indicate proton moving direction through water confined in the aggragates at forward and backward directions. The proton moving direction coincides with the axis along that each proton is shared according to the theoretical model [9].

However, in fact there is a deviation from the director that is due to proton hopping steps bypassing the neighboring water molecule [9]. So that the deviation is arisen because of proton moves along the tetrahedral network of hydrogen bonds surrounding the wires (or rods) of the TPP dimers contacting by phenyl rings [10]. As a result, the theoretical and experimental angles of the deviation of proton hopping steps relatively to the direction of proton moving (or director) were found to be 52.4°/2 = 26.2° and 55°/2 = 27.5° with the use of de-ionized water, respectively [9,12]. The less angle α = 43.2° is found for the aggregate in Figure 8B, when distilled water was used for the preparation of the assemblies that gives the less deviation, $\alpha/2$ = 21.6°. To quantify how much order is present in the material an order parameter (S) is defined as follows [5].

$$S = (1/2) \langle 3 \cos^2 \theta - 1 \rangle \quad (2)$$

where θ is orientational deviation of the molecules from the director, θ = $\alpha/2$. With θ =26.2°, 27.5°, and 21.6° the calculated orientational order parameters are S = 0.71, 0.68, and 0.797, respectively. With θ = $\alpha/2$ = 46.2°/2 for the ordered areas in Fig. 7 the calculated S = 0.769 that is close to S = 0.797. Thus, the three-component complex orientation is consistent with that of the wires (or rods) of the protonated TPP dimers of Figure 8. In both cases the distilled water was used for the preparation of the samples. The background of the SEM images (see Figure 8 and Appendix) attests the destroying of many nanoparticles in vacuum [10,12], so only the assemblies possessing a structure, which are covered by a thin metal film, are remained undestroyed on the plate in the vacuum.

Similar protons moving should take place during the crystallization process producing the particles of ellipsoid shape since they are formed in the thin layer under water vapor action on the self-organized domains. These particles found with a light Zeiss microscope are actually the micro-crystals [6]. The precursor of the microcrystal observed with contact AFM [6] is shown in Figure 9 which certainly has the crystalline appearance. Note that the bulk modulus (B_m) estimated for the microcrystals is found to be 3.72 GPa that is between B_m =12.7 GPa of the solid thin film, IR spectrum of which is shown in Figure 4, curve 1, and B_m =2.174 GPa of liquid water [6]. Hence, these particles produced by the precursors in the thin layer have been identified as liquid microcrystals.

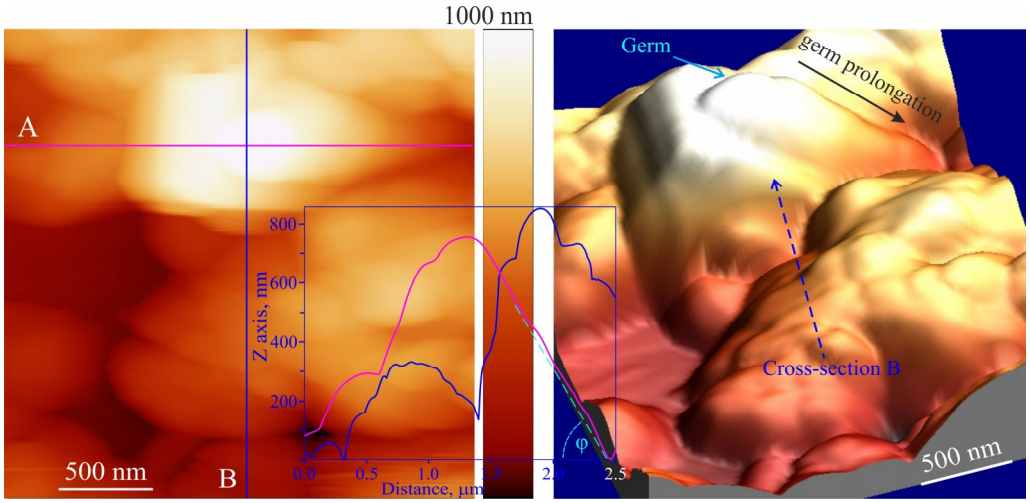

Figure 9. 2D image of microcrystal precursor obtained by contact AFM (2.5 μm×2.5 μm, top view, z–scale is 1000 nm) produced by the assembly of mono-protonated TPP dimers and water self-organized into domain after evaporation of 0.86 mol L^{-1} aqueous THF in the presence of 0.8 N HCl (to the left). Inset shows the cross-sections A and B, where A demonstrates the contact angle φ = 34–35°; and 3D image of the precursor exhibiting germ prolongation (to the right).

The final step of the crystallization process is the microcrystal precursor condensing, which is accompanied by disappearing of the prolongated part of the germ, while the germ located on the top

is remained unchanged. The precursor and the microcrystal both are shown in Figure 10, A and B, respectively. The precursor's facet, on which the prolongated part of the germ is located, has the contact (φ) angle of approximately 35° as displayed in Figure 9, inset, while the completely formed microcrystal shown in Figure 10B has the contact angle of 45.2° of the corresponding facet [6].

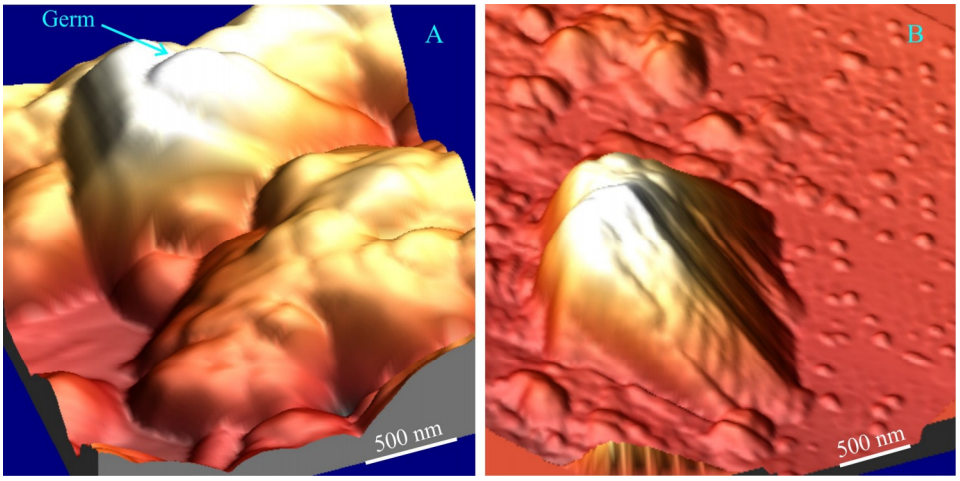

Figure 10. AFM image of: (A) the microcrystal precursor as displayed in Figure 9; and (B) the liquid microcrystal (3 μm×3 μm, top view, z–scale is 1300 nm) obtained by contact AFM after completion of the crystallization process. The self-organized assemblies consisting of mono-protonated TPP dimers and water were prepared like previously [6,16], i.e. in 0.86 mol L^{-1} THF with 0.8 N aqueous HCl.

Thus, the compression of the inner water-porphyrin matrix of the microcrystal precursor that is accompanied by the disappearance of the prolongated part of the germ occurs together with the action of the surface tension created by the aqueous surface layer, which gives larger contribution under the less contact angle.

3. Discussion

Water soluble organic solvents usually contain water as an admixture, so that even fresh distilled THF exhibits in IR spectrum a number of small bands like those in Figure 2, but not well resolved. Similar non-resolved small bands can be seen in IR spectrum of THF in Ref. [17] too. With the increase of water amounts in THF, these bands become well resolved and the most intense three-component 2680 cm^{-1} band attests the formation of the complex involving hydronium ion (H_3O^+) [7]. This three-component band matches a 2766 cm^{-1} band found in IR spectrum of a thin layer formed by the assemblies of protonated TPP dimers, which attests proton sharing in the N–H^+---O moiety of water cluster embedded between TPP units in the dimer [7]. The proton sharing is identified with a doublet nearby 1000 cm^{-1} observed in IR or resonance Raman spectra with an energy gap of 16–18 cm^{-1} or ca. 25 cm^{-1}, respecvitely [9,12]. Therefore, the characteristic 2680 cm^{-1} band attests proton sharing too but between oxygen atoms in the O---H^+–O moiety. In the sample of Figure 2, the H_2CO_3 acid has mainly been dissociated into ions H^+ and $(HCO_3)^-$, since the three-component 2680 cm^{-1} band is significantly larger in the magnitude than that at 3207 cm^{-1}. In contrast, as evidenced by the shoulder at 3200 cm^{-1} in the sample of Figure 1, inset (thin aqueous layer), the carbonic acid is present in the non-dissociated state, because of hydrochloric acid has not been evaporated under the sample preparation. As known in pure water, the majority of the CO_2 is not converted into carbonic acid because the hydration equilibrium constant ($K_{eq} = [H_2CO_3]/[CO_2]$) is ca. 1.7×10^{-3} at 298 K. Therefore, the three-component complex formation in the samples of Figures 1, inset and 2 is mainly caused by proton sharing arisen because of the hydrogen bonding. Thus, the structure of both these complexes should be the same including the O–O distance in the O---H^+–O

moiety, despite of the spectrum in Figure 1, inset exhibits the unstructured shoulder in the presence of a high concentration of hydrochloric acid.

It should be noted that proton sharing usually occurs between hydrogen-bonded water molecules in the excited state that requires an energy of 0.81422 eV in the case of vibrational mode of proton sharing [18,19]. Similar proton motion between the hydrogen-bonded molecules that is accompanied by the proton spin turnover as depicted in Scheme 1 requires considerably less energy, which occurs because of spin-orbit coupling between the electron and proton establishing the hydrogen bond [20]. In this case, the spin-orbit coupling parameter β = 1.19100654 is almost non-dependent on quaternary molecule coordination like under X-ray absorption [19]. Note that the O–O distance estimated above in the O---H$^+$–O moiety of the three-component complex is valid for similar complex formed in the presence of HCl because $R_{O–O}$ = 2.54 Å is defined by the spin-orbit coupling parameter but not ionized/non-ionized carboxyl group.

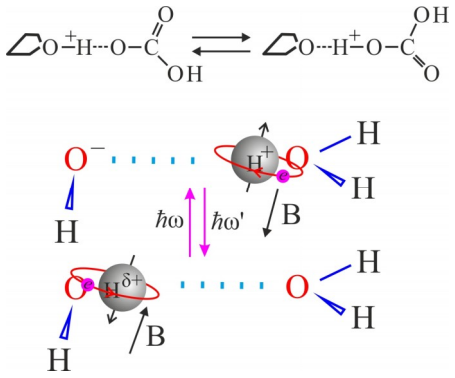

Scheme 1. Illustration of proton motion between the hydrogen-bonded water molecules accompanied by the change of the nucleus spin direction to the opposite resulting in the forward proton moving [20]. The difference ($\hbar\omega - \hbar\omega'$) = 1.41153 cm^{-1} arisen because of spin-spin interaction between the coupled proton and electron establishing the hydrogen bond is estimated with the hydrogen's Lamb shift [21]. Inset shows similar transitions in the moiety of THF and H_2CO_3 of the three-component complex.

Thus, in both cases the proton sharing provides hole polaron moving through water, which generates longitudinal optical (LO) photons in the case of the water-TPP molecular system [6,16]. The generation of LO phonons occurs even at 77 K in a vitreous solid [22] that implies the proton moving through water takes place in the film on the solid support of Figure 4, curve 1. While on the liquid support (Figure 4, curve 2), the proton collisions with oxygen atoms of water molecules generate the vibrations strongly increased in the magnitude.

An estimate of the frequency of proton sharing that takes place in the small-size protonated water cluster embedded between TPP units can be performed using characteristics of the doublet at 1000, 1025 cm^{-1} (Figure 3), where base line for the peaked bands is depicted by red. This small-size water cluster has hydrogen bonding connections with the network surrounding the TPP dimer [7]. Hence, the meta-stable resonance states are most likely depend on the oscillations of tetrahedral hydrogen bonds. As known, the width (Γ_{ms}) of the resonance produced by a meta-stable state is usually given by the relation, where τ_r is the lifetime of the resonance and $\hbar$ is the reduced Planck constant.

$$\Gamma_{ms} = \hbar/\tau_r \quad (3)$$

The width ($\Delta\nu_m$) measured for the meta-stable structure depicted in Figure 3, inset (to the right) is 21.786 cm^{-1}. To find proton sharing frequency, we should exclude spin-orbit coupling (namely $(\sqrt{\beta})^2$) for both electrons coupled with the same proton that is depicted in Scheme 1. Then $\Gamma_{ms} = \Delta\nu_m/\beta$ gives Γ_{ms} = 18.293 cm^{-1} (or 3.6338×10^{-22} J), and the calculated τ_r = 0.29021 ps. The latter is consistent with the period of hydrogen bonding oscillations of 0.2900212 ps [21], which is in fair agreement with the fast

Debye relaxation time τ_2 =182 fs of water [23] taking into account that the local levels are governed by factor $(R_{gold})^{-1}$ as evidenced in Ref. [21]. Thus, the calculated proton sharing frequency for liquid water ($f_{w,q} = \tau_r^{-1}$) with quaternary molecule coordination is that $f_{w,q}$ =3.4458 THz.

In contrast to the protonated TPP dimers contacting to each other via phenyl rings, the hydrogen atom or H^+ of the carbonic acid can easy change its location as depicted in Figure 4, inset. So the three-component complex formed between THF, $H_2CO_3/(HCO_3)^-$ and $(H_3O)^+$ can provide proton moving in forward and backward directions through the tight water of the ordered local area as displayed in Figure 7. However, this H/H^+ change should be accompanied by the change of two hydrogen bonds location in the structure. The latter occurs under proton motion between the hydrogen-bonded molecules with the change of proton spin direction to the opposite accompanied by an energy absorption producing so-called boson peak [20]. But if the change of proton spin direction occurs together with an excitation that results in the change of two hydrogen bonds location, then the absorbed energy should be less by $\hbar\omega'$ (see Scheme 1). Thus, for the proton moving through water in the solution with THF, the frequency of the absorbed energy can be evaluated theoretically using the frequency estimation in the case of boson peak. The following relation for a frequency ($f_{Hb} = c/\nu^{-1}$) absorption required for the proton motion along the direction between the hydrogen-bonded molecules was derived to explain the origination of boson peak [20].

$$f_{Hb} = [\hbar/(2\pi\, r_{ex}^2\, m_r^*)]\beta(g_e/g_p)(m^h_{ef}/m_p)\, m \qquad (4)$$

where r_{ex} is the polaronic exciton radius that is the average distance between the opposite charges, m_r^* is the reduced effective mass of polaronic exciton, $m_r^* = m^h_{ef}\, m^e_{ef}/(m^h_{ef} + m^e_{ef})$, m^h_{ef} and m^e_{ef} are respectively the effective masses of hole and electronic polarons, β is spin-orbit coupling parameter (β = 1.19100654 [19,20]), g_e and g_p are respectively the electron and proton g-factors, and m is quantum number. With r_{ex} =2.54 Å, g_e = 2.002319304, g_p = 5.5856947, $m^h_{ef} = 9.51m_e$, $m_p = 1836.152667m_e$, and m = 1 for proton, the calculated f_{Hb} =1.3294299 THz or ν_{Hb} =44.345 cm^{-1}. Effective masses of electronic ($m^e_{ef} = 0.5m_e$) and hole polarons ($m^h_{ef} = 9.51m_e$, m_e is the actual electron mass) in the condensed matter were discussed previously [16,22]. Then taking into account the wavenumber 2766 cm^{-1} characterizing proton sharing in the cluster between the protonated TPP dimers [7] and the energy $-(2\nu_{Hb}$ =2 × 44.345 cm^{-1}) diminishing the absorbed frequency per two hydrogen bonds in the case of the three-component complex, we arrive to 2677.31 cm^{-1} that is in fair agreement with the experimental 2680 cm^{-1}. While taking into account the difference $2(\hbar\omega - \hbar\omega')$ that is accumulated by the electron coupled with the proton [21], the estimation yields 2680.13 cm^{-1}.

The view on liquid crystal state is due to proton moving through water confined in a material in the absence of the diffusion of molecules is also supported by other experimental data, namely by a spectrum of porous silicon recorded in the transmittance mode [24]. The most intense three bands at 1012.3, 1081, and 1203 nm, wavelengths of which were calculated from the reported spectrum, characterize the intermolecular interactions in silicon microcavities. The first at 1012.3 nm (9878.4 cm^{-1}) attests O–H stretching vibrations of the hydrogen-bonded water molecules (3311.3 cm^{-1}) combined with vibrational mode of proton sharing (0.81422 eV, 6567.1 cm^{-1} [18]). Proton sharing is generated by appropriate frequency absorption by water in microcavities, therefore the second at 1081 nm (9250.5 cm^{-1}) should be a combination of proton sharing (6567.1 cm^{-1}) with the other vibration (2683 cm^{-1}) that is consistent with the experimental 2680 cm^{-1} displayed in Figure 2. The third band at 1203.5 nm (8308.5 cm^{-1}) attests the vibration of carboxyl groups (1741.4 cm^{-1}) combined with the proton sharing too (6567.1 cm^{-1}). A small band located at 1152.3 nm (8678.2 cm^{-1}) between two latter bands attests the proton sharing (6567.1 cm^{-1}) combined with the lowest Franck-Condon states of the electron coupled with the proton establishing the hydrogen bond. Namely, the frequency 2111 cm^{-1} (8678.2–6567.1) is close to 2127 cm^{-1} band observed in IR spectrum earlier [22]. While the energy of the lowest Franck-Condon transitions estimated with Fröhlich coupling constant is 2138 cm^{-1}. Hence, these four bands completely prove protons moving through water confined in the silicon microcavities. Thus, water and atmospheric CO_2 dissolved in water and

converted into carbonic acid, which filled the silicon's microcavities, form the pertinent matrix on the solid support that provides the liquid crystal state for a substance placed in the microcavities [24].

As mentioned above, the theoretical diviation from the director for the protonated TPP dimers, which contact to each other via their phenyl rings [10] forming the assemblies like wires or rods, is 52.4°/2 relatively to the proton moving direction. According to the model [9], the proton moving direction coincides with the direction of the proton momentum under its sharing between the hydrogen-bonded water molecules, so at the same time the director is the long axis of an aggregate. The sharp angle α = 43.2° observed for an aggregate in Figure 8 obtained with the use of distilled water is slightly less than that of 46. 2° found for the ordered areas of Figure 7. The sharp angle similarity implies similar molecular mechamism of proton hopping steps under its moving through water. On the other hand, it suggests that ionic admixtures in distilled water diminishes the deviation from the proton moving direction as compared with that in the case of de-ionized water when α = (55±3)° [12]. Thus, molecular characteristics of the three-component complex formed in aqueous THF due to the interaction of the dissolved carbon dioxide with water and of similar complex formed in the presence of HCl provide proton sharing in the O---H^+–O moiety. These characteristics are the O–O distance of 2.54 Å providing proton delocalization or proton moving through water and the orientational order parameter S = 0.769, which is obtained for the ordered areas of the tight water.

4. Materials and Methods

Synthesis of *meso*–tetraphenylporphine was carried out as described in Ref. [25]. Tetrahydrofuran and other organic solvents were of high-grade purity. Assemblies of protonated TPP dimers were produced in aqueous 0.8 N or 2 N HCl with 0.86 mol·L^{-1} THF by addition of the TPP solution to the aqueous HCl, the details in the relation to the TPP dimers self-assembling can be found elsewhere [7,16]. The preparation of thin layers was performed like previously [6,14]. Self-organized assemblies of mono-protonated TPP dimers were easy crystallized at relative humidity of 52–55%.

Infrared spectra of the samples in thin layer were recorded with a Specord M-80 spectrophotometer. Resonance Raman spectra of the self-assembled protonated TPP dimers in solution were obtained as described earlier [12]. Excitation was provided by a He-Cd laser with λ_{ex} = 441.6 nm mainly into the Soret band of di-protonated TPP dimer having λ_{max} = 437 nm. A spectral slit width of 4 cm^{-1} was used for the spectra recording. Contact AFM images were recorded with a Nanoscope II (Digital Instruments Inc.) at ambient conditions. A V-shaped cantilever of 200 μm length with a Si_3N_4 tip (spring constant 0.12 N m^{-1}) was used to probe the surface. Images of porphyrin assemblies were recorded in the height mode and the voltage was applied to the piezo elements, in order to keep the probing force constant for the topographic surface images.

Non contact AFM and simultaneous AFM/SNOM were applied in shear force mode with a Rasterscope™ 4000 and 2403 DualScope of Danish Micro Engineering (DME) with the use of 1.5 mm × 0.5 mm × 0.2 mm piezo elements. In SNOM, the surface was scanned by a light beam spreading through an optical fiber with the use of a helium-neon laser emitting 632.8 nm light. The feedback signal obtained from AFM was used for SNOM imaging. The variations of the light reflected back to the fiber SNOM setup under the shear-force AFM control provide SNOM image building up point by point. The working point was set close to 50% damping of the tip vibration and then optimized for best image quality. The tip was pulled with a Sutter Instrument, Model P-2000 Quartz Micropipette Puller [14]. The actual resolution of the obtained images was (10.3-10.6)±0.08 nm with the reliability of 99% estimated like previously [15]. Further details in the relation to AFM/SNOM measurements can be found in Ref. [26].

5. Conclusions

Summarizing the above results we can conclude that liquid crystal state of the self-organized assemblies of the protonated TPP dimers and water is created by tetrahedral network of hydrogen bonds fixed on the solid support, while protons shared in the O---H^+–O moieties can easy move through water confined in the assemblies. Hence, deviation of the orientaion of rod-like molecules or molecule wires from the director, which coincides with the long axis of an aggregate, is defined by molecular mechanism of proton moving through water confined in the material [9]. Then in addition to the TPP dimers providing proton moving through water [6,9,16], an organic solvent used for the dissolving of porphyrin and the porphyrin dimers self-assembling in the solution should maintain similar intermolecular interactions providing the proton sharing. The latter should take into the consideration that atmospheric CO_2 dissolved in water forms H_2CO_3 or $(HCO_3)^-$ and $(H_3O)^+$ ions. Alternatively, organic solvent interferes or prevents proton moving through water confined in the material, as a result of which microcrystals with the use of dioxane or dimethylformamide were not found excluding acetic acid. Thus, the physical nature of the formation of liquid crystal state deduced on the base of the results presented above admits liquid nanocrystals engineering too.

Acknowledgments: This work was supported in part by the Deutscher Akademischer Austauschdienst (DAAD), Ref. 325, Kennziffer: A/01/06685.

Conflicts of Interest: The author declares no conflict of interest. The founding sponsor had no role in the design of the study, in the collection, analyses, or interpretation of data, in the writing of the manuscript, and in the decision to publish the results.

Abbreviations

The following abbreviations are used in this manuscript:

AFM: Atomic Force Microscopy
LO phonon: longitudinal optical photon
SEM: Scanning Electron Microscopy
SNOM: Scanning Near-Field Optical Microscopy
TPP: *meso*-tetraphenylporphine
THF: tetrahydrofuran

Appendix

A thin metal film was deposited on the samples under vacuum for SEM experiments to avoid surface charging. Therefore, only the assemblies with hydrogen-bonded water molecules, which can self-organize into stable supramolecular structures, retain their form in the vacuum. Conversely, pollutions containing in water prevent the formation of continuous tetrahedral network of hydrogen bonds. As a result of the latter, such assemblies consisting of protonated TPP dimers and water with the admixtures of pollutions are unstable in vacuum [10,12] and were destroyed producing numerous remains like those displayed in Figure 11.

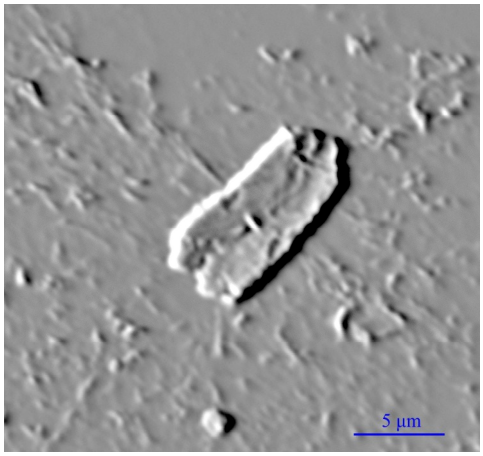

Figure 11. SEM image of the self-assembled mono-protonated TPP dimers and water obtained after evaporation of 0.86 ·⁻¹ aqueous THF in the presence of 0.4N HCl. The background contains numerous remains of the destroyed assemblies. The latter usually takes place on spring-time when water cannot be purified from the pollutions by the distillation.

References

1. Seideman, T. The liquid-crystalline blue phases. *Rep. Prog. Phys*. **1990**, *53*, 659–705.
2. Chandrasekhar, S. *Liquid Crystals*, 2nd ed.; Cambridge University Press: Cambridge, United Kingdom, 1992.
3. *Physical Properties of Liquid Crystals*, Demus, D., Goodby, J., Gray, G.W., Spiess H.-W., Vill V., Eds.; Wiley-VCH: Weinheim, Germany, 1999.
4. Rego, J.A.; Harvey, J.A.A.; MacKinnon, A.L.; Gatdula, E. Asymmetric synthesis of a highly soluble 'trimeric' analogue of the chiral nematic liquid crystal twist agent Merck S1011. *Liq. Cryst*. **2010**, *37*, 37–43.
5. Blinov, L.M. *Structure and Properties of Liquid Crystals*. Springer: Dordrecht-Heidelberg-London-NewYork, Germany-United Kingdom-USA, 2011.
6. Udal'tsov, A.V. Germ direct observation by AFM under crystallization of self-organized assemblies of mono-protonated *meso*-tetraphenylporphine dimers. *J. Crys. Growth*. **2016**, *448*, 6–16.
7. Udal'tsov, A.V. Microcrystals engineering using assemblies of di-protonated *meso*-tetraphenylporphine dimers under Zundel cations operation. *J. Mol. Struct.* **2015**, 1084, 308–318.
8. *New Developments in Liquid Crystals*. Tkachenko, G.V., Ed.; In-Teh: Vukovar, Croatia, 2009.
9. Udal'tsov, A.V.; Bolshakova, A.V.; Vos, J.G. The role of Zundel-like ions in the supramolecular self-organization of porphyrin assemblies. *J. Mol. Struct.* **2015**, 1080, 14–23.
10. Udal'tsov, A.V.; Kazarin, L.A.; Sweshnikov, A.A. Self-assembly of large-scale aggregates of porphyrin from its dimers and their absorption and luminescence properties. *J. Mol. Struct.* **2001**, *562*, 227–239.
11. Kulig, W.; Agmon, N. A 'cluster-in-liquid' method for calculating infrared spectra identifies the proton-transfer mode in acidic aqueous solution. *Nature Chem*. **2013**, *5*, 29–35.
12. Udal'tsov, A.V.; Bolshakova, A.V.; Vos, J.G. Highly ordered surface structure of large-scale porphyrin aggregates assembled from protonated TPP and water. *J. Mol. Struct.* **2014**, *1065–1066*, 170–178.
13. Udal'tsov, A.V.; Kazarin, L.A.; Sinani, V.A.; Sweshnikov, A.A. Water-porphyrin interactions and their influence on self-assembly of large-scale porphyrin aggregates. *J. Photochem. Photobiol. A: Chem*. **2002**, *151*, 105–119.
14. Udal'tsov, A.V.; Tosaka, M.; Kaupp, G. Microscopy of large-scale porphyrin aggregates formed from protonated TPP dimers in water-organic solutions. *J. Mol. Struct.* **2003**, *660*, 15–23.
15. Udal'tsov, A.V. Behavior of self-assembled Mn(III)/Mn(II)-NEt_3 conjugate on different support observed by AFM-SNOM, *J. Chem. Chem. Eng*. **2016**, *10*, 305–314.
16. Udal'tsov, A.V. Polaronic exciton in self-organized assemblies of protonated *meso*-tetraphenylporphine dimers and water at room temperature. *J. Mol. Struct.* **2016**, *1125*, 522–531.
17. Nakanishi, K. *Infrared Absorption Spectroscopy, Practical*. Holden-Day, Inc.: San Francisco, CA, USA, 1962.

18. Udal'tsov, A.V. Polaronic exciton and its energy levels in water structure. *J. Mol. Liquid*. **2017**, *227*, 262–267.
19. Udal'tsov, A.V. New insight into electronic neutrino creation under X-ray absorption by water tetrahedron intercalated with hydronium ion (H_3O^+). *J. Ener. Power Eng*. **2017**, *11*, 693–705.
20. Udal'tsov, A.V. Energy levels governed by golden section in O–H^+...O moiety under proton sharing coupled with spin-orbit interactions. *Vibr. Spectrosc*. **2018**, *97*, 16–23.
21. Udal'tsov, A.V. Gas-phase water: Features of hydrogen bonding deduced from far-infrared VRT spectra proving the cluster formation in vacuum. *Chem. Phys*. **2018**, 511, 46–53.
22. Udal'tsov, A.V. Hole polaron of small radius in assemblies of hydrated mono-protonated *meso*-tetraphenylporphine dimers at 77 K. *J. Phys. Chem. Solids* **2015**, *86*, 162–169.
23. Koeberg, M.; Wu, C.-C.; Kim, D.; Bonn, M. THz dielectric relaxation of ionic liquid: Water mixtures. *Chem. Phys. Lett*. 2007, *439*, 60–64.
24. Tkachenko, G.V.; Tkachenko, V.; Abbate, G.; De Stefano, L.; Rea, I.; Sukhoivanov, I.A. Nematic liquid crystal confined in electrochemically etched porous silicon: Optical characterization and applications in photonics, In *New Developments in Liquid Crystals*, Tkachenko, G.V., Ed.; In-Teh: Vukovar, Croatia, 2009; pp. 1–20.
25. Fuhrhop, J.-H.; Smith, K.M. Laboratory methods. In *Porphyrins and Metalloporphyrins*, Smith, K.M., Ed.; Elsevier: Amsterdam, The Netherlands, 1975, pp.757–869.
26. Kaupp, G. *Atomic force microscopy, scanning nearfield optical microscopy and nanoscratching*. Springer: Berlin-Heidelberg-Yew York, Germany-USA, 2006.